Structure and unexpected chiroptical properties of chiral 4-pyrrolidinyl substituted 2(5H)-furanones

ARTICLE *in* CHIRALITY · SEPTEMBER 2004

Impact Factor: 1.89 · DOI: 10.1002/chir.20059 · Source: PubMed

5 AUTHORS, INCLUDING:

Marcin Kwit
Adam Mickiewicz University
44 PUBLICATIONS **531** CITATIONS
SEE PROFILE

Karol Kacprzak
Adam Mickiewicz University
39 PUBLICATIONS **498** CITATIONS
SEE PROFILE

Urszula Rychlewska
Adam Mickiewicz University
186 PUBLICATIONS **1,631** CITATIONS
SEE PROFILE

CHIRALITY 16:405–413 (2004)

Structure and Unexpected Chiroptical Properties of Chiral 4-Pyrrolidinyl Substituted 2(5*H*)-Furanones

JACEK GAWROŃSKI,* KRYSTYNA GAWROŃSKA, MARCIN KWIT, KAROL KACPRZAK, AND URSZULA RYCHLEWSKA*
Department of Chemistry, A. Mickiewicz University, Poznan, Poland
Dedicated to the memory of Prof. R.H. Schlessinger

ABSTRACT Planar 2(5*H*)-furanones substituted at C4 with a chiral pyrrolidinyl group show CD spectra which are apparently due to the distortion of the C4-N1 bond of sp^2 character from the plane defined by the 2(5*H*)-furanone ring atoms and/or due to the presence of substituents in the pyrrolidine ring. This is a new, previously not encountered structural factor determining the chiroptical properties of 2(5*H*)-furanones and emerging from the analysis of X-ray diffraction data and quantum mechanical DFT computations. In the presence of a C5 pseudoaxial substituent in the furanone ring, the sign of the furanone $n-\pi^*$ and $\pi-\pi^*$ transition Cotton effects is determined primarily by the previously postulated allylic helicity rule. *Chirality 16:405–413, 2004.*

KEY WORDS: circular dichroism; X-ray structure determination; DFT computation

Chiral 2(5*H*)-furanones (butenolides) occur as natural products and are of great importance in diastereoselective synthesis.[1] They can be obtained by various synthetic protocols[2] and, in general, those obtained from natural sources or by methods involving enantioselective synthesis or by resolution of a racemate require determination of the absolute configuration. It has been demonstrated that in the case of 2(5*H*)-furanones having a stereogenic C5 atom a simple helicity rule allows prediction of their absolute configuration from the sign of the $\pi-\pi^*$ and $n-\pi^*$ Cotton effects (Fig. 1).[3,4]

The rule is based on two features of the butenolide structure: 1) the butenolide ring (the chromophore) is planar (achiral), 2) the presence of substituent $R^1 \neq H$ generates a helical bond system R^1-C-C=C, which is the determining factor of butenolide optical activity. Achiral substituents R^2 and R^3 do not appear to have an effect on the sign of the butenolide Cotton effects.

The rule has been applied to variously substituted butenolides with alkyl or alkoxy groups such as R^1 (alkoxy group contributing stronger than the alkyl group), with alkyl, alkoxy, thioalkyl, or halogen substituents such as R^2 and with alkyl, alkoxy, or halogen substituents such as R^3.[5] In all cases studied full consistency has been found between the signs of the observed Cotton effects and the absolute configuration of the C5 substituted 2(5*H*)-furanone, providing that the experimental $n-\pi^*$ and $\pi-\pi^*$ Cotton effects were correctly assigned.[5] Recently published CD data for substituted 2(5*H*)-furanones also conform to this rule.[6–10] 4-Pyrrolidinyl-substituted 2(5*H*)-furanones, such as **1b,** are apparent exceptions to the rule: the $\pi-\pi^*$ transition Cotton effect of **1b** at 272 nm is positive, rather than negative, as required by the rule.[5] Compounds of this type (also called vinylogous urethanes) with the chiral 4-pyrrolidinyl substituent (e.g., **2, 3, 7, 10**) have been widely used by Schlessinger's group as chiral auxiliaries in the synthesis of various natural products.[11–17] Knowledge of their conformation may be helpful in rationalizing the effect of asymmetric induction at C5 in the course of alkylation or aldol reactions. In addition, it is imperative to determine if the helicity rule for 2(5*H*)-furanones can be applied to 4-pyrrolidinyl-substituted derivatives (Structures 1).

It is well known that the structure of 4-amino-substituted 2(5*H*)-furanones can be best represented as a hybrid of the resonance forms **A, B** shown in Scheme 1.

There are two aspects of the structure relevant to the chiroptical properties discussed here: 1) the structures of the lowest energy conformers in equilibrium, and 2) the barrier to rotation around the C_{sp2}-N bond.

It is well documented that the basicity and the rotational barrier of cyclic enamines is related to the steric strain. Full delocalization of the nitrogen lone pair

Contract grant sponsor: Foundation for Polish Science (FNP) (to M.K. and K.K.)
*Correspondence to: J. Gawroński, Department of Chemistry, A. Mickiewicz University, 60780 Poznan, Poland. E-mail: gawronsk@amu.edu.pl, or U. Rychlewska. E-mail: urszular@amu.edu.pl
Received for publication 3 March 2004; Accepted 26 April 2004
DOI: 10.1002/chir.20059
Published online in Wiley InterScience (www.interscience.wiley.com).

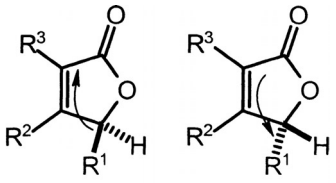

R^1–C–C=C helicity	*P*	*M*
n-π* Cotton effect	–	+
π-π* Cotton effect	+	–

Fig. 1. 2(5*H*)-Furanone helicity rule.

requires its orthogonality to the plane of the C=C bond. Less strained enaminoketones show a stronger conjugative interaction and higher barrier to rotation about the $C_{sp}2$-N bond. Thus, the order of the barriers is as follows: pyrrolidine > dialkylamine > piperidine substituent.[18] We reported previously that 2(5*H*)-furanones with 4-piperidinyl substituent display CD spectra conforming to the helicity rule, whereas those with the 4-benzylamino or 4-pyrrolidinyl substituent do not.[5] It is therefore reasonable to assume that 4-amino-substituted 2(5*H*)-furanones with a high rotational barrier constitute a new chromophoric system that is characterized by altered CD spectra. It is of interest to determine which of the structural factors is responsible for the induction of 4-amino-substituted butenolide Cotton effects.

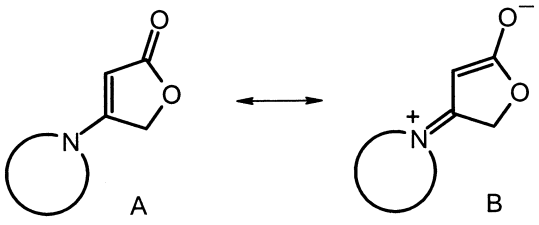

Scheme 1.

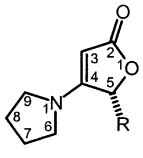

1a R = H
1b R = O(-)-menthyl

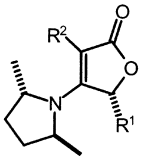

2 $R^1 = R^2 = H$
3 $R^1 = H$, $R^2 = Me$
4a $R^1 = Me$, $R^2 = H$
4b $R^1 = Et$, $R^2 = H$
4c $R^1 = CH_2CH{=}CH_2$, $R^2 = H$
5a $R^1 = R^2 = Me$
5b $R^1 = Et$, $R^2 = Me$

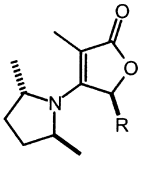

6a R = Me
6b R = $(CH_2)_2OH$

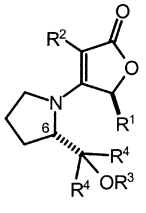

	R^1	R^2	R^3	R^4
7	H	H	Me	Me
8	H	Me	Me	Me
9	H	Me	H	Me
10	H	Me	TBS	Me
11	Me	Me	TBS	Me
12	H	Br	Me	Me
13	Me	Br	Me	Me
14	Me	*n*-Bu	Me	H

Structures 1.

EXPERIMENTAL

Compounds **2**,[19] *ent*-**3**,[19] **4b**,[19] **4c**,[19] **5**,[19] **6b**, **7**,[20] **8**, *ent*-**9**,[17] *ent*-**10**,[17] *ent*-**11**,[17] **12**,[20] and **13**[20] were obtained from Professor Richard H. Schlessinger and had the characteristics (m.p., $[\alpha]_D$) as reported. Compound **14** was obtained from Professor Kiyoharu Nishide.[21] The DFT computations were executed using the Gaussian 98 program.[22] CD/UV spectra were measured with a JASCO J-810 dichrograph.

X-Ray Data Collection, Solution, and Refinement of the Structures

The reflection intensities were measured on a four-circle *KM-4* (*KUMA Diffraction*) diffractometer with graphite monochromator.[23] Cu Kα radiation was used for compounds **2** and **3**, and Mo Kα radiation for compound **4b**. All measurements were performed at room temperature. The cell constants and the orientation matrix were obtained from a least-squares fit of at least 44 centered reflections. The reflections were measured using the ω-2Θ scan technique. Reflections for which $F^2 > 2\sigma(F^2)$ were considered as observed. The intensities were corrected for Lorentz and polarization effects; absorption corrections were not applied. The structures were solved by direct methods with SHELXS86[24] and refined with SHELXL97.[25] Heavy atoms (C, O, N) were refined anisotropically. The positions of the H-atoms were calculated and refined using a riding model with a common isotropic temperature factor. The absolute structure could not be reliably determined, therefore the Friedel pairs in the dataset were merged and not used as independent data. A Siemens Stereochemical Workstation was used to prepare drawings.[26] Crystal data and experimental details are summarized in Table 1. Crystallographic data (excluding structure factors) for structures **2**, **3**, and **4b** were deposited with the Cambridge Crystallographic Data Centre and allocated deposition numbers CCDC 231125–231127. Copies of the data can be obtained free of charge on application to the CCDC (12 Union Road, Cambridge

CB2 1EZ, UK; Fax: 44-1223-336-033. E-mail: deposit@ccdc.cam.ac.uk).

RESULTS AND DISCUSSION

Solid State Structure of 4-Pyrrolidinyl-Substituted 2(5H)-Furanones From X-ray Diffraction

Crystal data and experimental details for furanones **2, 3,** and **4b** are summarized in Table X (Experimental) and the molecules are illustrated in Figure 2. The characteristic features of the studied system discussed here: 1) planarity of the furanone ring; 2) puckering of the pyrrolidine ring; 3) mutual orientation of the two rings; 4) degree of pyramidalization of the nitrogen atom; and 5) degree of the conjugation in the O=C-C=C-N system of bonds.

In two of the three cases investigated (compounds **2** and **3**), the furanone ring is planar, with N1 being only 0.014(4) and 0.060(9) Å from the respective furanone planes. In **4b** and in its C3-methyl derivative **5b**[19] the furanone ring is slightly puckered, with C5 deviating most significantly from the five atom plane. This effect is apparently a result of the presence of the ethyl substituent at C5. However small, the effect of furanone ring puckering is more pronounced upon introduction at C5 of an alkyl (**4b, 5b**)[19] than an alkoxy substituent (**1b**).[5,27]

The degree of puckering of the pyrrolidine ring is the same in the three investigated compounds **2, 3,** and **4b,**

TABLE 1. Experimental details for X-ray diffraction study

Compound	2	3	4b
Crystal data			
Chemical formula	$C_{10}H_{15}NO_2$	$C_{11}H_{17}NO_2$	$C_{12}H_{19}NO_2$
Chemical formula weight	181.23	195.26	209.28
Cell setting	Orthorhombic	Orthorhombic	Orthorhombic
Space group	$P2_12_12_1$	$P2_12_12_1$	$P2_12_12_1$
a (Å)	8.865(2)	7.574(2)	8.327(2)
b (Å)	10.514(2)	8.921(2)	10.126(2)
c (Å)	10.653(2)	15.960(3)	13.888(3)
V (Å^3)	992.9(3)	1078.4(4)	1171.0(4)
Z	4	4	4
D_x (Mg m^{-3})	1.212	1.203	1.187
Radiation type	CuK_α	CuK_α	MoK_α
Wavelength	1.54178	1.54178	0.71073
No. of reflections for cell parameters	69	45	44
μ (mm^{-1})	0.681	0.661	0.080
Temperature (K)	293	293	293
Data collection			
Diffractometer	KM-4 four circle	KM-4 four circle	KM-4 four circle
Monochromator	Graphite	Graphite	Graphite
Data collection method	θ-2θ *scan*	θ-2θ *scan*	θ-2θ *scan*
No. of measured reflections	1712	1929	2101
No. of independent reflections	953	1079	1172
No. of observed reflections	750	493	834
Criterion for observed reflections	$I > 2\sigma(I)$	$I > 2\sigma(I)$	$I > 2\sigma(I)$
R_{int}	0.0735	0.0998	0.0293
θ_{max} (°)	63.08	64.96	24.71
Range of h, k, l	$-10 \rightarrow h \rightarrow 10$ $0 \rightarrow k \rightarrow 12$ $0 \rightarrow l \rightarrow 12$	$-8 \rightarrow h \rightarrow 8$ $0 \rightarrow k \rightarrow 10$ $0 \rightarrow l \rightarrow 18$	$-9 \rightarrow h \rightarrow 9$ $0 \rightarrow k \rightarrow 11$ $0 \rightarrow l \rightarrow 16$
Refinement			
Refinement on	F^2	F^2	F^2
$R[F^2 > 2\sigma(F^2)]$	3.97 %	5.10 %	3.61 %
$wR(F^2)$	9.68 %	16.79 %	10.56 %
S	1.077	0.979	1.018
No. of reflections used in refinement	953	1079	1172
No. of parameters used	119	128	137
H-atom treatment	Riding model	Riding model	Riding model
Weighting scheme	$w = 1/[\sigma^2(F_0^2) + (0.0463P)^2 + 0.0353P]$ where $P = (F_0^2+2F_c^2)/3$	$w = 1/[\sigma^2(F_0^2) + (0.0809P)^2 + 0.0297P]$ where $P = (F_0^2 + 2F_c^2)/3$	$w = 1/[\sigma^2(F_0^2) + (0.0615P)^2 + 0.1058P]$ where $P = (F_0^2+2F_c^2)/3$
$\Delta\rho_{max}$ (e Å^{-3})	−0.156	−0.159	−0.141
$\Delta\rho_{min}$ (e Å^{-3})	0.155	0.165	0.127

Computer programs used: data reduction: *KM4RED*; structure solution: *SHELXS86*; structure refinement: *SHELXL97*; preparation of material for publication: *SHELXL97*.

(a)

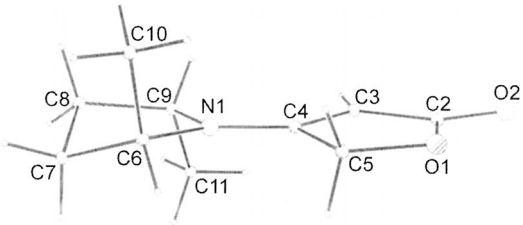

2

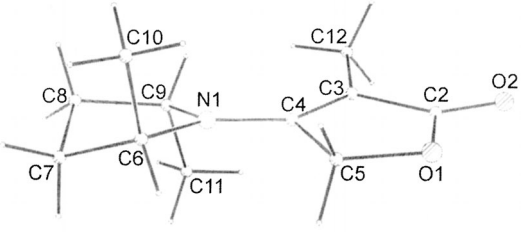

3

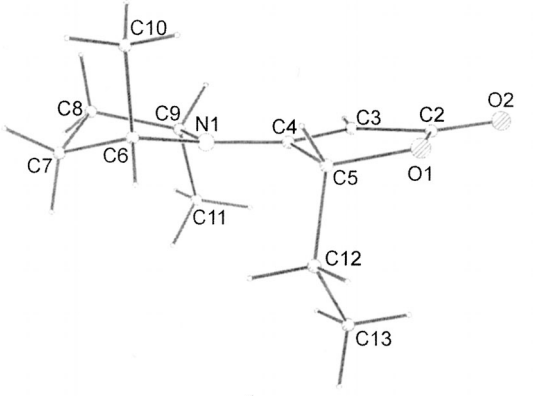

4

(b)

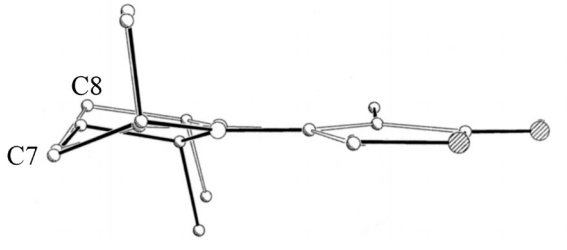

Fig. 2. a: Perspective view of 4-pyrrolidine-2(5*H*)-furanone derivatives **2, 3,** and **4b** studied by X-ray diffraction. **b:** Orthogonal fit of atoms of the furanone ring in **2** (open lines) and **3** (solid lines).

but the mode of puckering is different. In **2,** the pyrrolidine ring adopts the C7α-envelope conformation. Upon introduction of the methyl substituent at C3 (compound **3**), the pyrrolidine ring changes its conformation to C7α, C8β half-chair (see overlaid structures **2** and **3** in Fig. 2b). Similar tendency for conformational changes from an envelope to a half-chair upon methylation at C3 is observed for the analogous pair of compounds **4b** and **5b**.[19] Our previous results,[5] combined with the CSD search[27] of 4-pyrrolidine–2(5*H*)-furanone derivatives show that the unsubstituted pyrrolidine rings tend to be less puckered than their 2,5-dimethyl derivatives. In the former group the average torsion angle magnitude is in the range of 15.2–23.6°, while in the latter groups it varies from 24.7–27.1°.

Methyl substitution at C3 causes significant torsion around the C4-N1 bond. The C3-C4-N1-C9 torsion angle amounts to 1.6(6) and 13.4(9)° in **2** and **3,** respectively. In the analogous pair of derivatives, i.e., **4b** and **5b,**[19] this torsion angle adopts the value of 2.5 and 18.0°, again indicating a significant twist around the C4-N1 bond resulting from methyl substitution at C3. It might be worth noting that this torsion is in both cases positive. On the other hand, moderate negative twist around the C4-N1 bond is observed in **11** (−6.2°),[17] the negative sign of this torsion angle being related to the α-substitution at C6.

No pyramidalization of the nitrogen atom is observed in **2** and **3,** but in **4b** a slight pyramidalization does occur, as indicated by the sum of the valence angles around this nitrogen equal to 358.9°. A similar degree of nitrogen pyramidalization is observed in C5-disubstituted 4-pyrrolidine-2(5*H*)-furanone derivative,[20] while in **11**[17] it is substantially higher, as indicated by the sum of the valence angles equal to 357.5°.

There exists an extensive conjugation of the N1 lone pair, the C3=C4 double bond, and the C2 carbonyl bond. The geometrical consequence of this conjugation is a shortening of the N1-C4 bond to an average value in the three investigated compounds of 1.336(3)Å, which might be compared with the average value of 1.355(14) Å for the C-N bond in C=C-N-$(C)_2$ system.[28] The shortening of the N1-C4 bond is accompanied by the lengthening of the formally double C3=C4 bond to an average value of 1.352(6)Å, as compared with the value of 1.323(13)Å quoted for cyclopentene and with 1.340(13)Å in conjugated systems.[28] In the nonfused furanones deposited in the Cambridge Structural Database, CSD v. 5.24, updated July 2003,[27] the mean values of the three bond lengths in the C=C–C=O system of bonds equal to 1.341(39), 1.461(24), and 1.203(16) Å (391 observations, R < 7.5%). However, in 4-aminofuranones (12 observations, R < 7.5%) the mean values of the three bonds amount to 1.359(26), 1.433(20), and 1.216(11) Å, respectively. The two sets of values can be compared with the average values observed in the reported crystal structures **2, 3,** and **4b** 1.352(6), 1.431(12), and 1.206(9) Å, respectively. Interestingly, the mean value of the C(carbonyl)-O bond length 1.380(5)Å observed in the reported structures **2, 3,** and **4b** is significantly higher than the mean value of 1.369(23) and 1.369(14) Å for 2(5*H*)-furanone and 4-amino-2(5*H*)-furanone derivatives, respectively. The lengthening of the C(carbonyl)-O bond observed in the investigated crystal structures further supports the observation that the essential part of the electron delocalization is concentrated in the N1, C4, C3, C2, and O(2) region and that it takes place at the expense of delocalization within the ester function.

There is no reported example of the structure obtained by X-ray diffraction analysis which would be representa-

tive for compounds **8–10** and **12.** However, there are two structures reported, **11**[17] and a C5-disubstituted analog of **13,**[20] both having substituents at C3 and C5. A notable feature of these solid-state structures is the orientation of the pyrrolidinyl ring, with the bulky CMe_2OR substituent *syn,* i.e., on the side of the C3 methyl group. The pyrrolidinyl ring forms a C6β envelope in **11** whereas a C8α envelope is found in the analog of **13.** C4-N1 torsion angles are small and negative in these two compounds.

DFT Computations of the Structures

The structures of the 4-pyrrolidinyl-substituted 2(5*H*)-furanones **1a, 2, 3, 4a, 5a, 6a,** and **9** have been optimized by the DFT method at the b3lyp/6-311g(d, p) level. In all cases the conformers with pseudoaxial methyl or CMe_2OH groups in the pyrrolidine ring were found more stable ($\Delta E_{eq\text{-}ax} \geq 1.9$ kcal mol^{-1}), in accord with the structures determined by the X-ray diffraction studies. The calculated barrier to rotation around the C4-N1 bond in **1a** amounts to 18.4 kcal mol^{-1} and it is slightly lower in **2** (17.4 kcal mol^{-1}). Thus, there is a significant restriction of the rotational freedom around the bond joining the two heterocycles. Furthermore, while the slope of the free energy curve for **1** is symmetrical, with E_{max} at $\alpha = 90°$ (as expected), it is unsymmetrical in the case of **2,** with E_{max} at $\alpha = 100°$ due to the chirality of the pyrrolidinyl substituent (Fig. 3).

The computed lowest-energy conformers of **1a–6a** and **9** had a planar 2(5*H*)-furanone ring and a C7α envelope conformation of the pyrrolidine ring. Additionally, they were characterized by the torsion angle C3-C4-N1-C9, as shown in Table 2. The pattern of changes of the torsion angle matches well the data obtained from X-ray diffraction analysis for compounds **2, 3, 4b, 5b,** and **11.** Thus, only a very small torsion angle is calculated for **1a** and intermediate torsion angle values were obtained for C3-unsubstituted butenolides **2** and **4a.** On the other hand, introduction of a C3 methyl group causes a significant increase of the torsion angle to nearly 20° (butenolides **3** and **5a**), regardless of the presence of a methyl substituent in C5α position. It can be concluded that the large

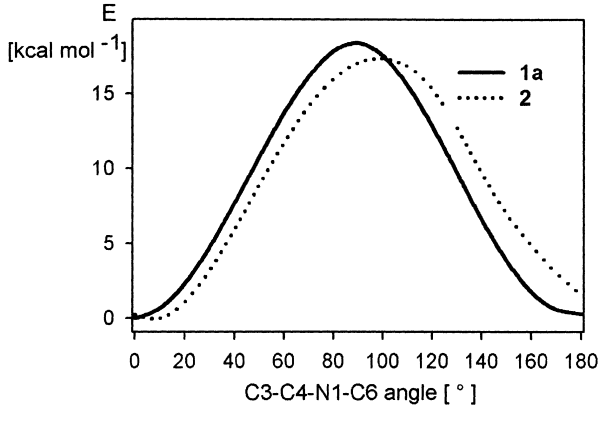

Fig. 3. Computed barrier to rotation around C4-N1 bond in 4-pyrrolidine- 2(5*H*)-furanones **1a** and **2**.

TABLE 2. Computed and X-ray diffraction determined C3-C4-N1-C9 torsion angles (°) in 4-pyrrolidine-2(5*H*)-furanones

	1a	**2**	**3**	**4a**	**4b**	**5a**	**5b**	**6a**	**9***anti*	**9***syn*	**11**
DFT	0	6.1	19.8	5.7	—	18.7	—	11.2	172	−0.2	—
X-ray	—	1.6	13.4	—	2.5	—	18.0	—	—	—	−6.2

C4-N1 torsion angle is primarily due to the presence of a substituent (Me, Br) in C3 position. However, the torsion angle is reduced (as in **6a**) when there is a competitive interaction of the pyrrolidinyl ring with both C3 and C5β substituents.

Our DFT computations gave but a single low-energy conformer for each butenolide **1a–6a.** However, in the case of **9** two low-energy conformers, **9***anti* and **9***syn*, were found, the latter having 0.85 kcal mol^{-1} higher energy (Structures 2). In both conformers the calculated torsion angle around the C4-N1 bond is small and negative (−8° in **9***anti* and −0.2° in **9***syn*), despite seemingly large steric effects due to the CMe_2OH substituent in the *syn* conformer. Here the effect of the C3 methyl group on the magnitude of the C4-N1 torsion angle appears less pronounced, apparently as a result of unsymmetrical substitution of the pyrrolidine ring.

*Circular Dichroism of 4-Pyrrolidinyl-Substituted 2(5***H***)-Furanones*

4-Pyrrolidinyl-substituted 2(5*H*)-furanones **2–14** display two Cotton effects in the 200–300 nm range of the CD spectra. The long-wavelength Cotton effect at 270–285 nm (in methanol solution) is of π–π* type and corresponds to UV_{max} ($\epsilon > 20{,}000$). The short-wavelength Cotton effect is of n–π* type and is located at 212–235 nm (no corresponding UV_{max}) (Table 3).[29]

The large blue shift of the n–π* band relative to the π–π* band in 4-amino-substituted 2(5*H*)-furanones has been reported previously.[5] It is well known that the position of the UV_{max} of 2(5*H*)-furanones is red-shifted by introduction of substituents at C3 and C4, as well as by an increase of polarity of the solvent, i.e., a batochromic shift is caused by alkyl or heterosubstituents at C3 and C4 as well as by the increase of polarity of the solvent. In addition to the data published,[5] we note that 4-pyrrolidinyl substituent (as in **2** and **7**) shifts the UV_{max} to 266–269 nm

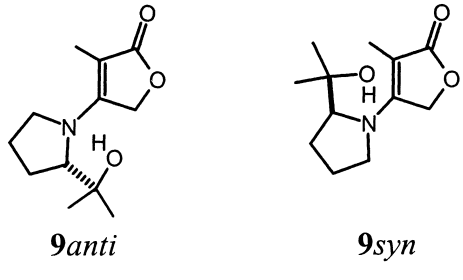

9*anti* **9***syn*

Structures 2.

TABLE 3. CD/UV data for 4-pyrrolidine-2(5*H*)-furanones in methanol solution

Compound	Δε (nm) π-π*	Δε (nm) n-π*	ε (nm)
(6*S*,9*S*)-**2**	−8.8 (270)	−2.5 (223)	28 800 (269)
(6*S*,9*S*)-**3**	−15.8 (279)	+4.4 (215)	25 500 (278)
(5*R*,6*S*,9*S*)-**4b**	−14.8 (272)	2.6 (229)	25 300 (272)
(5*R*,6*S*,9*S*)-**4c**	−13.2 (271)	−2.3 (218)	23 600 (272)
(5*S*,6*S*,9*S*)-**6b**	+26.9 (282)	−12.6 (219)	22 500 (282)
(6*S*)-**7**	+2.5 (270)	−0.7 (235)	23 300 (266)
(6*S*)-**8**	+26.7 (278)	−9.5 (212)[a]	25 200 (278)
(6*S*)-**9**	+23.8 (276)	−7.5 (214)	25 100 (277)
(6*S*)-**10**	+24.5 (277)	−10.6 (214)	22 100 (278)
(5*S*,6*S*)-**11**	+27.5 (283)	−8.4 (213)	22 200 (280)
(6*S*)-**12**	+18.6 (286)	−12.3 (218)	20 400 (282)
(5*S*,6*S*)-**13**	+19.3 (285)	−12.1 (218)	21 400 (282)
(5*S*,6*S*)-**14**	+12.2 (280)	−6.0 (215)	20 400 (277)

[a]Shoulder.

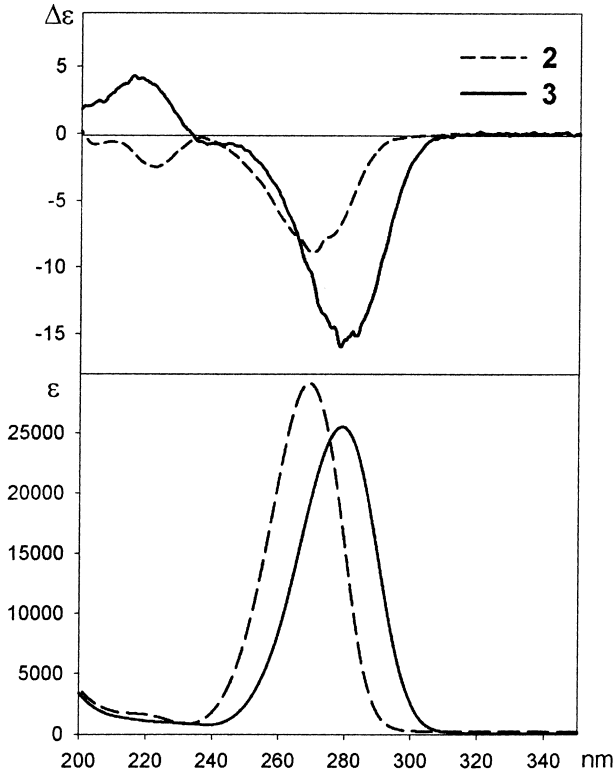

Fig. 4. CD (upper panel) and UV (lower panel) spectra of 4-pyrrolidine-2(5*H*)-furanones **2** and **3**.

(in methanol). Methyl and bromo substituents at C3 contribute to the red-shift of the UV_{max} by ~10 nm and 15 nm, accordingly. Additional red shift (2–4 nm) is due to an alkyl substituent at C5 (see for example **4b**). The effect of substitution at the allylic position on the position of UV_{max} has not been previously considered; the present data suggest that allylic substituents, such as alkyl groups, should also be treated as contributing weakly to the excitation energy of the π−π* transition of the butenolide chromophore.

The π−π* and n−π* Cotton effects of compounds listed in Table 3 have opposite sign (as expected), except for **2** and **4c.** Majority of vinylogous urethanes listed in Table 3 show substantial Cotton effects, even in the absence of an allylic alkyl substituent; however, two vinylogous urethanes **2** and **7,** which lack substituents at C3 and C5, display only relatively weak Cotton effects. In these molecules the chiral 4-pyrrolidinyl substituent is sterically least encumbered and the C4-N1 bond is least deformed from planarity (see data in Table 2). When substituent is present in the allylic (C5) position (**4b, 4c, 6b, 11, 13, 14**), the signs of the π−π* and n−π* (except for **4c**) Cotton effects conform to the butenolide helicity rule.

More intriguing is the origin of the Cotton effects of the butenolides having no substituent at C5 (**2, 3, 7–10, 12**). Representative CD/UV spectra of butenolides **2, 3, 7,** and **8** are shown in Figures 4 and 5. It is significant to note that the π−π* Cotton effects of butenolides substituted with pyrrolidines of opposite configuration (**2** or **3** vs. **7** or **8**) are also of opposite sign. The π−π* Cotton effects of **2** and **3** at 270 and 279 nm, respectively, are of the same sign (negative). In the case of **7** and **8** they are also of the same sign (positive), but the Cotton effect of **7** is one order of magnitude weaker compared to that of **8.** The X-ray structural and DFT computational data (Table 2) provide a possible explanation for the different CD behavior due to C3 methyl substitution. The important difference between the structures of **2** and **3** is the degree of twist of the conjugated enamino lactone chromophore. While the O=C-C=C bond system is planar in **2** and **3,** there is a significant twist around the C4-N1 bond in **3** and only a small one in **2.** A similar C4-N1 bond twist angle difference is seen between the pairs of structures **4a/5a** and **4b/5b.** The larger twist angle around the C4-N bond in **3** and **5a, 5b** is due to the steric effect of the C3 methyl group; N1-C9 bond is pushed down from the plane defined by C2, C3 and C4 atoms (see Fig. 2b). Thus, the strong negative π−π* transition Cotton effects of **3** is correlated with the positive twist angle of C4-N1 bond. The (weaker) negative π−π* Cotton effect of **2** can be explained on a similar structural basis.

Excited states and rotational strengths of the lowest-energy conformers of **2** and **3** were computed at the b3lyp/6-311++g(d, p) level in order to compare with the experimental data (Fig. 6). For **2** the most intense π−π* transition was computed at 246 nm and it had a negative rotational strength, just as had the CD band of **2** at 270 nm. It should be noted that the 24-nm difference between the calculated and experimental λ_{max} merely reflects a strong solvent effect on the stabilization of highly polar excited state of the π−π* transition. This can be compared with a 7-nm blue shift of the CD band of **2** when measured in hexane solution.[29] For **3,** calculations provided the expected red-shift of the π−π* absorption band, λ_{max} at 258 nm, due to C3 methyl substitution. The computed rotational strength for this transition was also negative, in agreement with the experimental Cotton effect. We note that the red-shift of the π−π* absorption

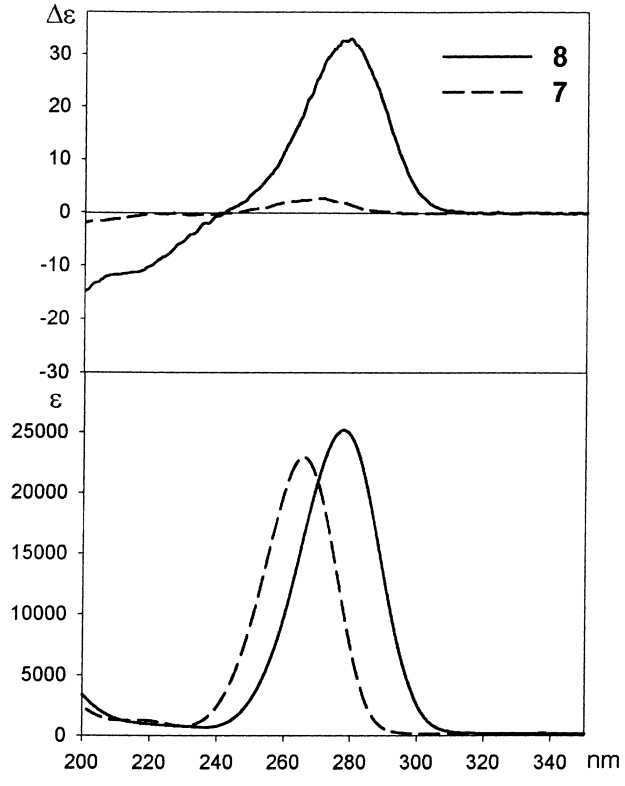

Fig. 5. CD (upper panel) and UV (lower panel) spectra of 4-pyrrolidine-2(5*H*)-furanones **7** and **8**.

band due to substitution at C3 may originate from a steric effect of the substituent, causing a deformation of the C4-N1 bond from planarity. Thus, the computed positions of the $\pi-\pi^*$ transition in conformers of **1a** having the C3-C4-N1-C9 torsion angle of 0° and 20° are correspondingly at 234 nm and 244 nm. This links the batochromic shift of the $\pi-\pi^*$ transition with nonplanarity of the C4-N1 bond.

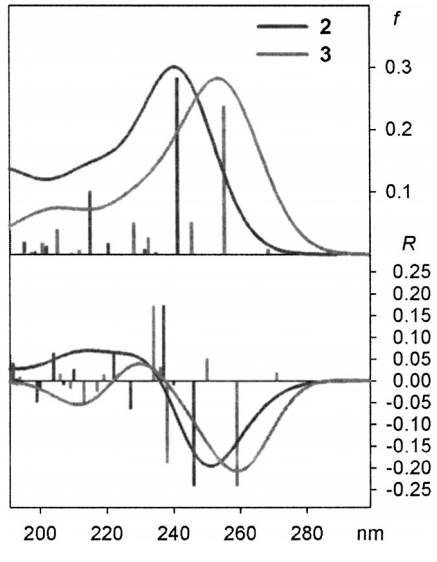

Fig. 6. Computed UV (upper panel) and CD (lower panel) spectra of 4-pyrrolidine-2(5*H*)-furanones **2** and **3**.

In the case of the two DFT computed conformers **9***anti* and **9***syn* the computations at the b3lyp/6-31+g(d,p) level provided a positive rotational strength for the long-wavelength (250 nm) $\pi-\pi^*$ transition (Fig. 7). The computed rotational strength was much higher in the case of **9***anti*, apparently due to a larger negative C4-N1 torsion angle in this conformer, as compared to that of **9***syn* (see below).

It should be added, however, that the effect of a chiral 4-pyrrolidinyl substituent on the CD spectra may not be exclusively due to deformation from planarity of the C4-N1 bond. Under dynamic conformational equilibrium other factors are likely to contribute, such as the presence of pyrrolidine ring substituents (Me or CMe_2OR) in pseudoaxial positions as well as pyrrolidine C-C bonds which are not coplanar with the plane of the butenolide ring. Although the majority of the structures characterized either by X-ray diffraction or by DFT computations were pyrrolidine C7α envelope conformers, other conformers, such as C8β half-chair or, in the case of **11** and an analog of **13,** C6β or C8α envelopes have also been identified. This makes analysis of the CD spectra even more complicated. We computed the CD spectra of 2(5*H*)-furanones **2** and **3** in their lowest-energy conformations (as shown in Fig. 6) and then used the same conformers with the pyrrolidine methyl groups substituted by hydrogen atoms to compute the CD spectra of such demethylated analogs (demethylated **2** is a skewed conformer of **1a**). Due to the (negative) skew angle the C4-N1 bond the demethylated molecules are chiral and their CD spectra can be compared with those of **2** and **3** (see Fig. 8). As shown in Figure 8, the long-wavelength Cotton effect of demethylated **2** is less intense compared to **2,** but the opposite relation is seen in the case of **3** and its

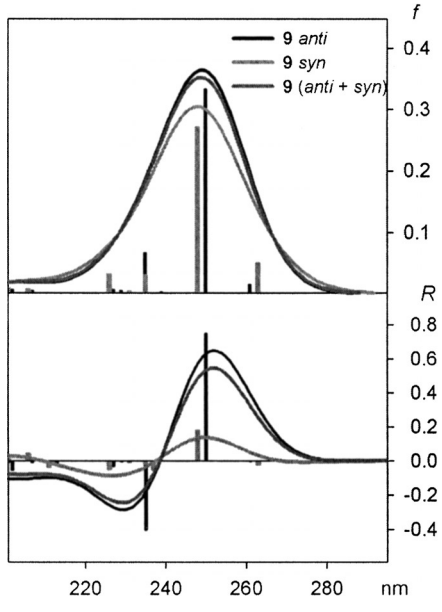

Fig. 7. Computed UV (upper panel) and CD (lower panel) spectra of conformers **9***anti* and **9***syn*, as well as for **9** with Boltzmann distribution of conformers at 298 K.

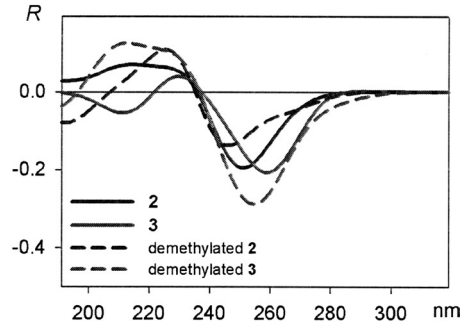

Fig. 8. Comparison of computed CD spectra of 4-pyrrolidine-2(5*H*)-furanones **2** and **3** and their 6,9-demethylated analogs.

demethylated analog. The effect of pyrrolidine ring substituents on the CD spectra of 2(5*H*)-furanones cannot be neglected; however, at present it is difficult to assess its sign and magnitude.

CONCLUSION

Our work demonstrates, through the combined use of X-ray diffraction structure determination and quantum mechanical DFT computations, that in an achiral chromophore, such as 2(5*H*)-furanone, the optical activity is generated by introducing either of the two chiral perturbers: 1) an allylic pseudoaxial substituent, or 2) the twist of the formally single C-N bond of the pyrrolidine substituent. This substituent extends the conjugation of the chromophore through cyanine-type delocalization of the donor electron pair of the pyrrolidine nitrogen atom. The former case has been previously well documented and summarized as a helicity rule, shown in Figure 1. The latter is a new observation for the conjugated enamino carbonyl chromophores in which the amino part has a relatively high rotational barrier due to extended conjugation with the π system. While the present study does not provide a simple correlation between the structure of chiral pyrrolidine substituted 2(5*H*)-furanones and their CD spectra, it nevertheless indicates possible factors responsible for this relationship. One is deviation from planarity of the C4-N1 bond participating in π-electron delocalization. A reverse relationship has been established: positive rotational strength of the $\pi-\pi^*$ Cotton effect corresponds to a negative torsion angle around the C4-N1 bond. Other possible factors involve rotational contributions from C-C bonds in the pyrrolidine ring which are not coplanar with the plane of 2(5*H*)-furanone ring.

LITERATURE CITED

1. a) Hanessian S, Murray PJ. Stereochemical control of nature's biosynthetic pathways: a general strategy for the synthesis of polypropionate-derived structural units from a single chiral progenitor. Tetrahedron 1987;43:5055–5072. b) Feringa BL, de Lange B, Jansen JFGA, de Jong JC, Lubben M, Faber WS, Schudde EP. New approaches in asymmetric synthesis using γ-alkoxybutenolides. Pure Appl Chem 1992;64:1865–1871.
2. a) Van Oeveren A, Feringa BL. Asymmetric synthesis of 5-substituted γ-lactones and butenolides via nucleophilic addition to oxycarbenium ions derived from 5(*R*)-(menthyloxy)-4(*R*)-(phenylsulfanyl)-2(*3H*)-dihydrofuranone. J Org Chem 1996;61:2920–2921. b) Faber WS, Kok J, de Lange B, Feringa BL. Catalytic kinetic resolution of 5-alkoxy-2(*5H*)-furanones. Tetrahedron 1994;5:4775–4794. c) Toda F, Tanaka K, Leung CW, Meetsma A, Feringa BL. Preparation of optically active 5-alkoxyfuran-2(*5H*)-ones and 5-methoxydihydrofuran-2(*3H*)-one by chiral inclusion complexation. J Chem Soc Chem Commun 1994:2371–2372. d) Van der Deen H, Hof RP, van Oeveren A, Feringa BL, Kellog RM. Lipase catalyzed enantioselective transestrification of 5-acyloxy-2(*5H*)-furanones. Tetrahedron Lett 1994;35:8441–8444. e) Trost BM, Müller TJJ. Butenolide synthesis based upon a contraelectronic addition in a ruthenium-catalyzed Alder ene reaction. Synthesis and absolute configuration of (+)-ancepsenolide. J Am Chem Soc 1994;116:4985–4986.
3. Gawronski JK, van Oeveren A, van der Deen H, Leung CW, Feringa BL. Simple circular dichroic method for the determination of absolute configuration of 5-substituted 2(*5H*)-furanones. J Org Chem 1996;61:1513–1515.
4. Uchida I, Kuriyama K. $\pi-\pi^*$ circular dichroism of α,β-unsaturated γ-lactones. Tetrahedron Lett 1974;43:3761–3764.
5. Gawroński JK, Chen QH, Geng Z, Huang B, Martin MR, Mateo AI, Brzostowska M, Rychlewska U, Feringa BL. Chiroptical properties, structure, and absolute configuration of heterosubstituted 2(*5H*)-furanones. Chirality 1997;9:537–544.
6. König GM, Wright AD, Bernardinelli G. Determination of the absolute configuration of a series of halogenated furanones from the marine alga *Delisea pulchra*. Helv Chim Acta 1995;78:758–764.
7. Drioli S, Felluga F, Forzato C, Nitti P, Pitacco G, Valentin E. Synthesis of (+)- and (−)-phaseolinic acid by combination of enzymatic hydrolysis and chemical transformations with revision of the absolute configuration of the natural product. J Org Chem 1998;63:2385–2388.
8. Zanardi F, Battistini L, Rassu G, Auzzas L, Pinna L, Marzocchi L, Acquotti D, Casiraghi G. The utility of furan-, pyrrole-, and thiophene-based 2-silyloxy dienes as demonstrated by modular synthesis of annonaceous acetogenin core units and their pyrrolidine and thiolane analogues. J Org Chem 2000;65:2048–2064.
9. Soriente A, Crispino A, De Rosa M, De Rosa S, Scettri A, Scognamiglio G, Villano R, Sodano G. Stereochemistry of antiinflammatory marine sesterterpenes. Eur J Org Chem 2000;947–953.
10. Ma S, Wu S. Novel CuX_2-mediated cyclization of acid-base salts of (L)-cinchonidine or (D)/(L)-a-methylbenzylamine and 2,3-allenoic acids in an aqueous medium. An efficient entry to optically active β-halobutenolides. Chem Commun 2001;441–442.
11. Schlessinger RH, Gillman KW. An enantioselective solution towards synthesizing "skip" 1,3-dimethyl stereocenters. A synthesis of 4*S*(2*E*, 4*R**, 6*R**)-4,6-dimethyl-2-octenoic acid. Tetrahedron Lett 1996;37:1331–1334.
12. Schlessinger RH, Li Y-J. Total synthesis of (−)-virginiamycin M_2 using second-generation vinylogous urethane chemistry. J Am Chem Soc 1996;118:3301–3302.
13. Schlessinger RH, Li Y-J, von Langen DJ. Nonracemic *syn*-selective aldol reactions with a second-generation vinylogous urethane lithium enolate. J Org Chem 1996;61:3226–3229.
14. a) Dankwardt SM, Dankwardt JW, Schlessinger RH. A vinylogous urethane approach towards the synthesis of okadaic acid. Construction of the C1-C8 fragment. Tetrahedron Lett 1998;39:4971–4974. b) Dankwardt SM, Dankwardt JW, Schlessinger RH. A vinylogous urethane approach towards the synthesis of okadaic acid. Construction of the C9-C18 fragment. II. Tetrahedron Lett 1998;39:4975–4978. c) Dankwardt JW, Dankwardt SM, Schlessinger RH. Synthesis of the C19 through C27 segment of okadaic acid using vinylogous urethane aldol chemistry. III. Tetrahedron Lett 1998;39:4979–4982. d) Dankwardt JW, Dankwardt SM, Schlessinger RH. Synthesis of the C28 through C38 segment of okadaic acid using vinylogous urethane aldol chemistry. IV. Tetrahedron Lett 1998;39:4983–4986.
15. Schlessinger RH, Pettus LH. Asymmetric *syn*-selective aldol reaction of γ-oxygenated vinylogous urethane with a second generation chiral auxiliary: application in construction of (+)-3-deoxy-D-*manno*-2-octulosonic acid. J Org Chem 1998;63:9089–9094.
16. Schlessinger RH, Gillman KW. Asymmetric total synthesis of

(+)-phomalactone, (+)-acetylphomalactone and (+)-asperlin utilizing a novel *syn*-selective C_4-oxa-vinylogous urethane. Tetrahedron Lett 1999;40:1257–1260.

17. Schlessinger RH, Mjalli AMM, Adams AD. An approach to erythronolide A seco acid via a simple tetronic acid. J Org Chem 1992;57: 2992–2993.
18. Cook AG, Absi ML, Bowden VK. Basicity of some mono- and bicyclic enamines and tricyclenamines. J Org Chem 1995;60:3169–3171.
19. Schlessinger RH, Iwanowicz EJ, Springer JP. Highly diastereoselective alkylation reactions of vinylogous urethanes derived from simple tetronic acids. Tetrahedron Lett 1988;29:1489–1492.
20. Schlessinger RH, Pettus TRR, Springer JP, Hoogsteen K. Diastereoselective Diels-Alder reactions using furan substituted with a nonracemic amine. J Org Chem 1994;59:3246–3247.
21. Nishide K, Aramata A, Kamanaka T, Inoue T, Node M. Total asymmetric syntheses of (+)-blastmycinone and related γ-lactones. Tetrahedron 1994;50:8337–8346.
22. Frisch MJ, Trucks GW, Schlegel HB, Scuseria GE, Robb MA, Cheeseman JR, Zakrzewski VG, Montgomery Jr JA , Stratmann RE, Burant JC, Dapprich S, Millam JM, Daniels AD, Kudin KN, Strain MC, Farkas O, Tomasi J, Barone V, Cossi M, Cammi R, Mennucci B, Pomelli C, Adamo C, Clifford S, Ochterski J, Petersson GA, Ayala PY, Cui Q, Morokuma K, Malick DK, Rabuck AD, Raghavachari K, Foresman JB, Cioslowski J, Ortiz JV, Baboul AG, Stefanov BB, Liu G, Liashenko A, Piskorz P, Komaromi I, Gomperts R, Martin RL, Fox DJ, Keith T, Al-Laham MA, Peng CY, Gill A, Nanayakkara C, Gonzalez M, Challacombe PMW, Johnson B, Chen W, Wong MW, Andres JL, Gonzalez C, Head-Gordon M, Replogle ES, Pople JA. Gaussian 98; Gaussian, Inc.: Pittsburgh, PA; 1998.
23. Gałdecki Z, Kowalski A, Uszyński L. DATAPROC data processing program. Version 9. Kuma Diffraction, Wrocław, Poland; 1999.
24. Sheldrick GM. Phase annealing in SHELX-90: direct methods for larger structures. Acta Cryst 1990;A46:467–473.
25. Sheldrick GM. SHELXL97 program for the refinement of crystal structures. University of Göttingen; 1997.
26. Stereochemical Workstation Operation Manual, Release 3.4. Siemens Analytical X-Ray Instruments, Inc., Madison, WI; 1989.
27. Allen FH, Kennard O. Chemical Design Automation News 1993;8:1, 31–37.
28. Orphen AG, Brammer L, Allen FH, Kennard O, Watson DG, Taylor R. Typical interatomic distances in organic compounds and organometallic compounds and coordination complexes of the d- and f-block metals. In: Burgi HB, Dunitz JD, editors. Structure correlation. Wienheim: VCH; 1994. 2:751–858.
29. We have also recorded the CD/UV spectra of samples dissolved in hexane. The main differences can be summarized as follows: the ϵ_{max} values are lower in hexane solution, yet the $\pi-\pi^*$ Cotton effects are stronger. As expected, the λ_{max} of the $\pi-\pi^*$ transition is blue-shifted and the position of the $n-\pi^*$ Cotton effect is red-shifted, compared to those recorded for methanol solution.